Vascular Channel Formation by Human Melanoma Cells *in Vivo* and *in Vitro*: Vasculogenic Mimicry

Andrew J. Maniotis,*† Robert Folberg,†‡§
Angela Hess,* Elisabeth A. Seftor,*†
Lynn M.G. Gardner,‡ Jacob Pe'er,¶
Jeffrey M. Trent,‖ Paul S. Meltzer,‖ and
Mary J. C. Hendrix*†

From the Departments of Anatomy and Cell Biology,* University of Iowa Cancer Center;† and the Departments of Ophthalmology and Visual Sciences‡ and Pathology,§ University of Iowa College of Medicine, Iowa City, Iowa; the Department of Ophthalmology,¶ Hadassah University Hospital, Jerusalem, Israel; and the Cancer Genetics Branch, National Human Genome Research Institute, National Institutes of Health, Bethesda, Maryland‖

Tissue sections from aggressive human intraocular (uveal) and metastatic cutaneous melanomas generally lack evidence of significant necrosis and contain patterned networks of interconnected loops of extracellular matrix. The matrix that forms these loops or networks may be solid or hollow. Red blood cells have been detected within the hollow channel components of this patterned matrix histologically, and these vascular channel networks have been detected in human tumors angiographically. Endothelial cells were not identified within these matrix-embedded channels by light microscopy, by transmission electron microscopy, or by using an immunohistochemical panel of endothelial cell markers (Factor VIII-related antigen, Ulex, CD31, CD34, and KDR[Flk-1]). Highly invasive primary and metastatic human melanoma cells formed patterned solid and hollow matrix channels (seen in tissue sections of aggressive primary and metastatic human melanomas) in three-dimensional cultures containing Matrigel or dilute Type I collagen, without endothelial cells or fibroblasts. These tumor cell-generated patterned channels conducted dye, highlighting looping patterns visualized angiographically in human tumors. Neither normal melanocytes nor poorly invasive melanoma cells generated these patterned channels *in vitro* under identical culture conditions, even after the addition of conditioned medium from metastatic pattern-forming melanoma cells, soluble growth factors, or regimes of hypoxia. Highly invasive and metastatic human melanoma cells, but not poorly invasive melanoma cells, contracted and remodeled floating hydrated gels, providing a biomechanical explanation for the generation of microvessels *in vitro*. cDNA microarray analysis of

highly invasive *versus* poorly invasive melanoma tumor cells confirmed a genetic reversion to a pluripotent embryonic-like genotype in the highly aggressive melanoma cells. These observations strongly suggest that aggressive melanoma cells may generate vascular channels that facilitate tumor perfusion independent of tumor angiogenesis. *(Am J Pathol 1999, 155:739–752)*

It is generally assumed that tumors require a blood supply for growth and metastasis.[1] The development of the tumor microcirculation compartment includes both the production of new blood vessels (angiogenesis) and their remodeling.[2] In fact, the number of vessels[3] and the patterning of the microcirculation[4] by remodeling events are used as histological markers of tumor progression. Although attention has been focused on factors that stimulate and suppress tumor angiogenesis, the molecular mechanisms underlying tumor remodeling remain enigmatic. It is therefore critical to investigate remodeling of the intratumoral microvasculature in various tumor models.

Melanoma is among the better characterized tumor models with respect to prognostic staging of disease progression. The rising incidence of cutaneous melanoma makes this tumor an important public health problem. Melanoma of the interior of the eye, uveal melanoma, although much less common than cutaneous melanoma, poses a threat to vision and significant morbidity; nearly 50% of patients with uveal melanoma die from metastatic melanoma.[5] Cutaneous melanoma may disseminate through lymphatics or blood vessels. In contrast, the interior of the eye lacks lymphatics, and uveal melanoma, which develops in one of the most capillary-rich tissues of the body, is a paradigm for pure hematogeneous dissemination of cancer.[6] Therefore, the development of a tumor microcirculation in uveal melanoma is a rate-limiting step for hematological metastasis and serves as an important model for study of the cellular and molecular infrastruc-

ture of the melanoma microvasculature, isolated from the influence of a concomitant lymphatic circulation.

The objective of this investigation was to elucidate the relationship between the aggressive melanoma cell phenotype and the mechanisms responsible for the generation of uniquely patterned matrix-associated vascular channels characteristic of both aggressive human uveal and cutaneous melanomas.

Materials and Methods

Light Microscopy

To highlight the matrix-associated vascular channels of uveal melanomas, tissues were stained with periodic acid-Schiff (PAS), omitting hematoxylin counterstaining to reduce visual noise; black and white photography with a green filter (or the selection of the green channel for digital photography) further highlighted the PAS-positive patterns.[7] Failure to eliminate hematoxylin counterstaining to the PAS stain has resulted in a 50% reduction in the histological detection of PAS-positive looping patterns and networks.[8]

The prognostic significance of the presence of PAS-positive patterns in uveal melanoma was tested by us on a series of 234 patients whose eyes had been removed for uveal melanoma. Details concerning the composition of patients in this data set and statistical analyses were reported elsewhere. Briefly, the primary outcome variables were the time to death from metastatic melanoma or from other causes and the time to follow-up for those patients who were still alive. The analyses focused on time to death from metastatic melanoma. We treated time to death from other causes, time to follow-up for living patients, and time to last contact for patients reported as lost to follow-up as censored times in the data analyses.[4,9,10]

Correlations with Indocyanine Green Angiography

A series of 18 patients with choroidal melanoma were studied prospectively with indocyanine green angiography using a confocal scanning laser ophthalmoscope (Heidelberg Retinal Angiograph, Heidelberg Engineering, Heidelberg, Germany)[11–13]; two of these patients had their eyes removed following the angiogram. The eyes were fixed in 10% neutral buffered formalin for at least 48 hours, and opened via a coronal incision through the pars plana to allow for direct visualization of the tumor surface[14] and to enhance an accurate correlation with retinal landmarks by comparison with pre-enucleation fundus photographs and the confocal angiographs. Each tumor was sectioned through the zone corresponding to the intratumoral microcirculation as seen on the angiograms. Sections were stained using the modified PAS without hematoxylin stain. Details of the prospective study and the angiographic-histological correlations were reported elsewhere.[13]

Transmission Electron Microscopy

Human tissue samples and cultures were fixed initially in 10% neutral buffered formalin. One half of the tumor sample was processed for diagnostic light microscopy and stained with the PAS stain without hematoxylin counterstaining. Areas of tumor containing PAS-positive looping patterns were identified and were used to map and microdissect areas of tumor containing these patterns from wet tissue corresponding to the opposite face of tissue embedded in paraffin. These small regions of tumor were postfixed in 2.5% buffered glutaraldehyde and were postfixed further in a solution of 1% osmium tetroxide, dehydrated, and embedded in a standard fashion. Thin sections were stained with uranyl acetate-lead citrate and examined with a Hitachi S-7000 transmission electron microscope.

Immunohistochemistry

For light microscopic immunohistochemistry, paraffin sections were cut at 4 to 5 μm. Slides were deparaffinized using xylene and absolute ethanol, rinsed in distilled water, exposed to proteinase K for 2 minutes or antigen unmasking. (The antigen unmasking solution was heated in a steamer to 95°C, then cooled to 75°C before slides were placed in it.) The solution and slides were heated in an oven at 65°C for 55 minutes. For Ulex (Vector Laboratories, Burlingame, CA), Factor VIII-related antigen (Dako, Carpenteria, CA), CD31 (Dako), and KDR (Flk-1; Santa Cruz Biotechnology, Santa Cruz, CA), slides were placed in either PBS or Tris-buffered saline, pH 7.4 (TBS, Sigma Chemical Co., St. Louis, MO). The sections were rinsed with phosphate-buffered saline (PBS) and blocked subsequently with 10% normal horse serum in PBS. Sections were stained with the appropriate primary antibody or lectin for 1.5 hours, then incubated for 20 minutes (10 minutes for KDR) with biotinylated anti-rabbit or anti-mouse immunoglobulins in PBS. This was followed by incubation with streptavidin (Zymed, South San Francisco, CA) conjugated to alkaline phosphatase in PBS for 20 minutes, then by a brief rinse in distilled water. Sections were exposed to Vector red chromogen (Vector Laboratories) for up to 2 minutes, an enhancement solution (Zymed) for 5 minutes, rinsed in distilled water, counterstained with Mayer's hematoxylin for 8 minutes, and coverslipped with a permanent mounting medium. For CD34 (Novocastro, Vector Laboratories), antigen unmasking was followed by staining with the CD34 for 30 minutes, washing in Tris buffer, then placement into Envision Polymer (Dako) for 30 minutes and washing with Tris buffer. Sections were exposed to Vector red chromogen for up to 2 minutes, washed in distilled water, counterstained with Mayer's hematoxylin for 8 minutes, and coverslipped with permanent mounting media.

Dual immunofluorescence labeling of keratins 8 and 18 and vimentin IFs was accomplished using antikeratin antibodies CK-5, (Sigma) conjugated with Oregon Green (Molecular Probes, Eugene, OR) for keratins, and V.9 (Dako) conjugated with Texas Red-X (Molecular Probes)

for vimentin, as previously described,[15] All coverslips were observed with either a Zeiss LSM410 (Thornwood, NY) or Bio-Rad (Hercules, CA) 1024 laser scanning confocal microscope, and the images digitized using either the Zeiss KS400 or Bio-Rad Confocal Assistant V. 3.10 software packages.

Dual immunohistochemistry labeling of CD31 and S-100 protein was accomplished using an antibody to CD31 as described above, followed by application of a serum blocking solution (Zymed) for 15 minutes. Sections were then exposed to antibody to S-100 protein (Dako) for 1.75 hours followed by washing with PBS-Tween Gold-conjugated secondary antibody (Zymed) which was diluted by 50% in PBS and applied for 30 minutes. Sections were then washed in PBS-Tween and were exposed to a silver enhancer (Zymed) for 10 minutes, followed by a wash in PBS-Tween. The sections were then counterstained with Mayer's hematoxylin for 8 minutes and coverslipped with permanent mounting medium. These sections were viewed by direct light microscopy to detect CD31 and by epipolarization microscopy to detect the S-100 protein signal.

Cell Culture

Cell lines derived from primary choroidal or ciliary body melanomas or from foci of metastatic uveal melanoma to the liver[16] and normal melanocytes, as described previously,[17] as well as the human cutaneous metastatic melanoma cell line C8161,[18] were maintained in Dulbecco's modified Eagle's medium (DMEM, Life Technologies, Gaithersburg, MD) supplemented with 10% fetal bovine serum (FBS, Gemini Bioproducts, Calabasas, CA).[19] Endothelial cells derived from pulmonary, brain, and dermal microvasculature (HMEC-1), HUVECs, and embryonic chick endothelial cells were maintained in DMEM, 20% FBS, or 1× MITO+ (Collaborative Biomedical, Bedford, MA).[20,21] Cell cultures were determined to be free of mycoplasma contamination using the GenProbe rapid detection system (Fisher, Itasca, IL).

Three-Dimensional Cultures

Twelve microliters of Matrigel or Type I collagen (Collaborative Biomedical) were dropped onto glass coverslips and allowed to polymerize for 1 hour at 37°C. Tumor cell lines, normal uveal melanocytes, or endothelial cells were then seeded on top of the gels at high density and allowed to incubate. For conditioned media experiments, media were collected and passaged through a 0.2-μm filter before being placed on the appropriate cells. Addition of conditioned media-soluble factors (basic fibroblast growth factor (bFGF), transforming growth factor (TGF)-β, vascular endothelial growth factor (VEGF), platelet-derived growth factor (PDGF), and tumor necrosis factor (TNF)-α, all from Sigma) or antibodies to $\alpha_v\beta_3$ or α_v (Chemicon, Temecula, CA) was performed by pretreatment and continuous treatment regimes during the 1- to 2-week incubation period in 3D cultures (Table 1).

Invasion Assay

Tumor cells (1×10^5) were seeded into the upper wells of the MICS (membrane invasion culture system) chamber[22] onto collagen/laminin/gelatin-coated (Sigma) polycarbonate membranes containing 10-μm pores (Osmonics, Livermore, CA) in DMEM containing 1× MITO+ (Collaborative Biochemical). After 24 hours of incubation at 37°C, the cells that invaded each membrane were collected, stained, and counted as previously described.[23] Percent invasion was corrected for proliferation and calculated as follows:

$$\frac{\text{total number of invading cells}}{\text{total number of cells seeded}} \times 100$$

Micromanipulation and Microinjection

For micromanipulation, an Eppendorf workstation was used with a second Leitz manipulator, and morphological alterations were quantitatively recorded with a video recording device and measured with NIH Image software.[24] For microinjections, Texas Red (Molecular Probes) was preloaded into short barrel pipettes pulled on a Sutter pipette puller, delivered into large sinusoidal channels, and observed continuously for 30 minutes.

In Vitro Collagen Lattice Deformation Assays

Floating collagen lattices[25] were prepared by placing a 250-μl drop of the collagen-cell suspension (0.65 mg/ml of Collagen I (Collaborative Biomedical) and 1.25×10^5 cells/ml) in a bacteriological 35-mm Petri dishes to prevent adhesion of the gel to the culture substrate. After 1 hour at 37°C to allow polymerization of the collagen, 1.6 ml of complete medium was placed over the collagen lattice. Lattice contraction was quantified as the relative change in the gel diameter over time, using NIH Image software. Rhodamine 123 dye (Molecular Probes) was incubated with melanoma cells for 18 hours and washed before cells were placed on floating gels to demonstrate the distribution of tumor cells in contracting gels.

Microarray Analysis

cDNA microarrays detected altered gene expression in highly invasive melanoma cells by a method previously described.[26] Relative expression of selected genes critical for vascular channel formation is reported (Table 2) as highly invasive and metastatic *versus* poorly invasive uveal melanoma cells. Hybridization to cDNA microarrays followed the previously described procedures[27] (see also http://www.nhgri.nih.gov/DIR/LCG/15K/HTML/). Briefly, RNA extracted from poorly invasive and highly invasive/metastatic melanoma cells was converted to cDNA in the presence of fluorescent nucleotides Cy3- or Cy5-dUTP. The labeled cDNA pools were mixed and hybridized to microarrays containing 5000 cDNA elements selected from the Unigene database.[28] Fluorescence intensities for each gene were measured with a

custom instrument, and ratios were calculated as described.[27]

Results

Histology of the Melanoma Microcirculation, its Prognostic Significance, and in Vivo Functional Correlations

Many melanomas enlarge within the uvea without containing prominent zones of necrosis (Figure 1A). In our series of 234 eyes removed for malignant melanoma of the choroid or ciliary body, we discovered that 106 (45%) tumors contained networks of interconnected PAS-positive back-to-back loops (Figure 1B).[4] Uveal melanoma tends to spread first and preferentially to the liver,[29] and we discovered that liver metastases from uveal melanomas also contained these patterns (Figure 1C), as did foci of metastatic uveal melanoma in other organ sites.[16] We have also detected PAS-positive loops and networks in metastatic cutaneous melanoma (Figure 1D).

By conventional hematoxylin-eosin stains and with high magnification, the PAS-positive loops were seen to have a solid component in some areas which splayed open to reveal hollow channels, some of which contained red blood cells; these channels also connected to somewhat larger vascular spaces containing red blood cells (Figure 1E). Light microscopy revealed that the interior of these hollow channels, red blood cell-containing channels, and vascular spaces was not lined by an endothelium.

We studied the prognostic significance of the PAS-positive patterned matrix-associated vascular channels in a group of 234 patients whose eyes were removed for uveal melanoma. The histological presence of loops or networks had a stronger association with death from metastatic melanoma, in a multivariate Cox proportional hazards model, than all other conventional histological features studied, including tumor size, cell type, and mitotic activity.[4,9,10] There was a strong statistical separation in survival between patients whose tumors lacked loops and networks and those whose tumors contained these patterns (Figure 1F). The statistical association between the histological presence of microcirculatory loops and networks and death from metastatic melanoma has been confirmed by independent laboratories.[8,30,31] We found subsequently that loops and networks are not found in uveal nevi,[32] that networks tend to localize preferentially to the periphery of the tumor (the tumor growth zone),[33] that the amount of tumor remodeling by looping patterns (the percentage of area occupied by these patterns on a two-dimensional tissue section) had a negative effect on patient survival,[10] and that the classification of tumors into high- and low-risk for metastasis was likely to be consistent regardless of the tissue plane sampled within a large tumor.[34]

These PAS-positive patterns were presumed to be associated with the tumor microcirculation for several reasons. First, PAS-positive patterns connect in tissue sections with vascular spaces containing red blood cells (Figure 1, B and C). Second, PAS-positive networks were traced in serial sections to connect with the vortex vein, which drains the choroid.[6] Third, the patterns splay open and contain red blood cells (Figure 1E). Fourth, comparisons of adjacent tissue sections stained alternately with PAS and with Ulex europaeus agglutinin I showed histological correspondence between PAS-positive patterns with Ulex staining.[7] Finally, three-dimensional reconstructions by laser scanning confocal microscopy of thick melanoma tissue sections stained with Ulex revealed anastomosing tubular and sinusoidal structures, consistent with vascular channels.[6,35]

The ability to directly visualize the circulation of blood in a tumor in the absence of lymphatics makes the angiographic study of intraocular melanoma an ideal venue for investigating the functional perfusion of the patterned matrix-associated vascular channels in patients. Two patients from a series of 18 patients whose uveal melanomas were imaged clinically with this technique had their eyes removed after confocal angiography. One of these patients showed angiographic evidence of loops forming networks within the tumor (Figure 1G), and we detected PAS-positive network patterns in histological sections taken from this area of the tumor (Figure 1H). The other patient had angiographic evidence of only large, pre-existing choroidal vessels within the tumor (an absence of loops, Figure 1I) and showed only normal choroidal vessels histologically and no looping patterns (Figure 1J).[13] Unlike cutaneous melanoma, which is usually accessible to biopsy without major morbidity, it is difficult to obtain representative quantities of tumor tissue from within the eye for histopathological analysis without risking compromise to vision. Thus, the ability of ophthalmologists to image prognostically significant microcirculatory patterns clinically in patients by confocal angiography or by ultrasound power spectrum analysis[36] provides noninvasive substitutes for biopsy.

Transmission Electron Microscopy of Melanoma Microcirculation Patterns

By light microscopy, patterned matrix-associated vascular channels containing red blood cells did not appear to be lined by endothelium. We therefore microdissected tissue sections from uveal melanomas to isolate tumor tissue containing PAS-positive loops and networks of loops (Figure 2A). Ultrastructurally, these vascular channels were not lined by endothelium but were delimited by a thin basal lamina and were lined externally by tumor cells (Figure 2B) containing premelanosomes and melanosomes (Figure 2C). These ultrastructural findings confirmed the light microscopic observations that melanoma cells were associated with these vascular channels and were situated on the outer surface of the tubular wall (Figure 2D) rather than internal, as would be expected of an endothelial lining. The presence of a basal lamina lining the vessel wall correlated with the PAS-positive staining of the patterned matrix in tissue sections. The PAS stain is used routinely in ophthalmic pathology to facilitate identification of critical intraocular basement
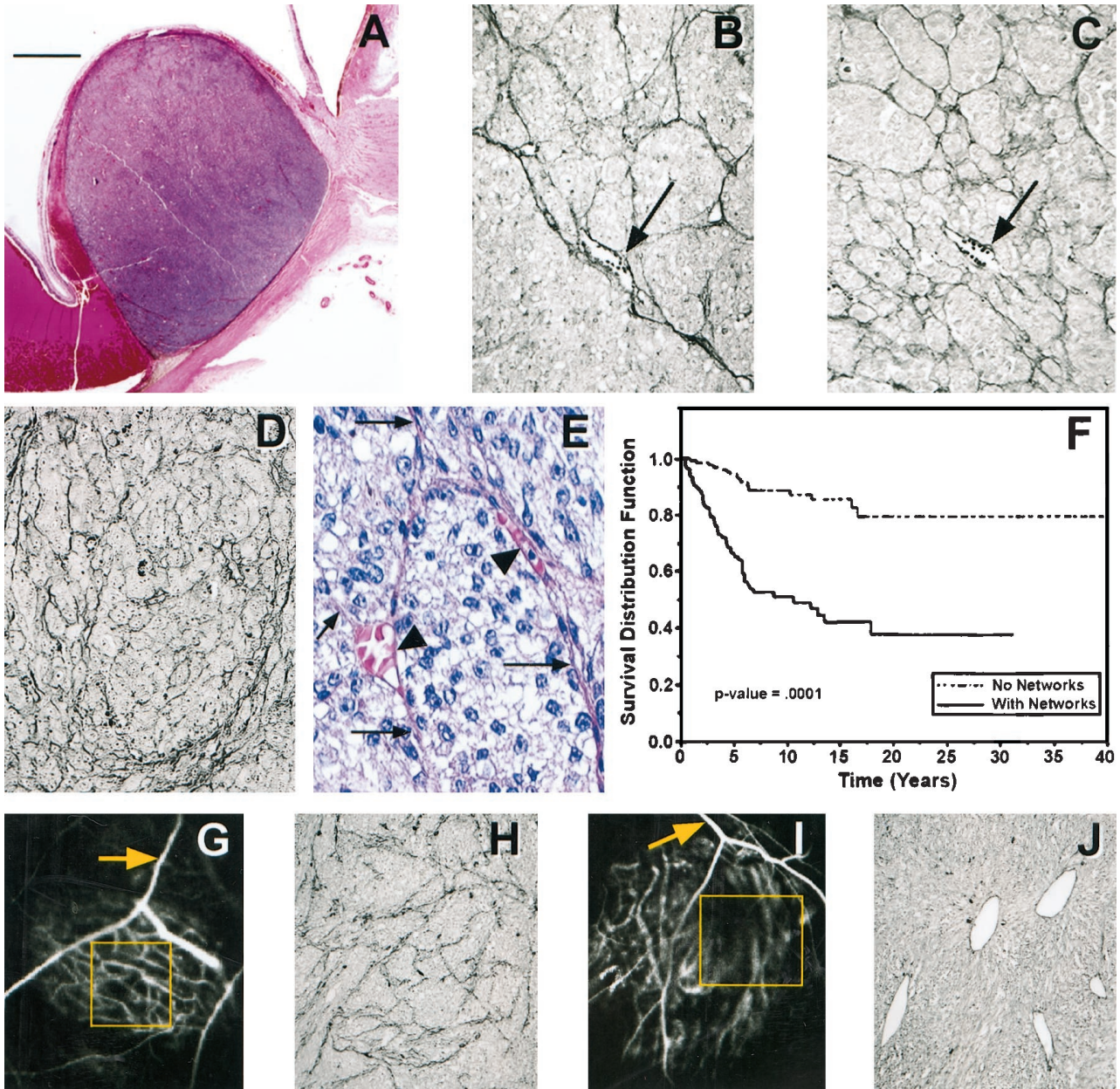
Figure 1. Histology of the melanoma microcirculation, its prognostic significance, and *in vivo* functional correlations. **A:** Primary uveal melanoma in the choroid of a patient who died of metastatic melanoma 3 years after the eye was removed. Note the absence of necrosis. Hematoxylin-eosin stain; scale bar, 2 mm. **B:** Light microscopic view of PAS-stained tissue sections of primary human uveal melanoma (**arrow** demonstrates a sinusoid with red blood cells). **C:** Uveal melanoma metastatic to the liver, showing patterns of interconnected loops forming networks anastomosing to sinusoids (**arrow**) containing red blood cells. **D:** PAS-stained histological section of metastatic cutaneous melanoma containing multiple networks. **E:** Hematoxylin-eosin stained section of primary uveal melanoma; the structures corresponding to the PAS-positive components of loops and networks consist of solid cords (**arrows**) that connect to round channels or tubes containing red blood cells (**arrowheads**). Note that these tubules are lined externally by melanoma cells and no endothelial cells are identified. **F:** Kaplan-Meier survival curves for deaths from metastatic uveal melanoma: melanomas without networks *versus* melanomas with networks (after Folberg, et al[4]). **G:** Angiogram of uveal melanoma taken after intravenous injection of indocyanine green and photographed with a laser scanning confocal ophthalmic recording device.[11] The vessels forming an inverted "Y," highlighted by the yellow arrow, are within the retina. The anastomosing loops between the two inverted branches of the "Y" formed by the retinal vessels and enclosed by the yellow box are deeper within the tumor and represent the microcirculation of this melanoma. This eye was subsequently removed and studied histologically[13] (shown in **H**). **H:** Tissue section stained by PAS, without hematoxylin counterstain, taken from the tumor at the location enclosed by the box from the angiogram (**G**). Many PAS-positive loops forming networks are seen in this tissue, corresponding precisely to the loops seen in the angiogram. **I:** Angiogram of uveal melanoma taken after intravenous injection of indocyanine green and photographed with a laser scanning confocal ophthalmic recording device.[11] In contrast to the angiogram shown in **G**, looping vessels are not seen within the tumor (yellow box). The vessels within the tumor are parallel straight vessels. This eye was subsequently removed and studied histologically[13] (shown in **J**). **J:** Tissue section stained by PAS without hematoxylin taken from the area in the tumor enclosed by the box on the angiogram (**I**). Dilated normal choroidal vessels are identified and correspond to the straight parallel vessels on the angiogram. Scale bar, 2 mm (**A**). Original magnifications, ×40 (**B, C, H, J**), ×80 (**D**), ×120 **E**. Tissue stains: hematoxylin-eosin (**A** and **E**), PAS without hematoxylin counterstaining, photographed with a green filter (**B-D, H-J**).[7]
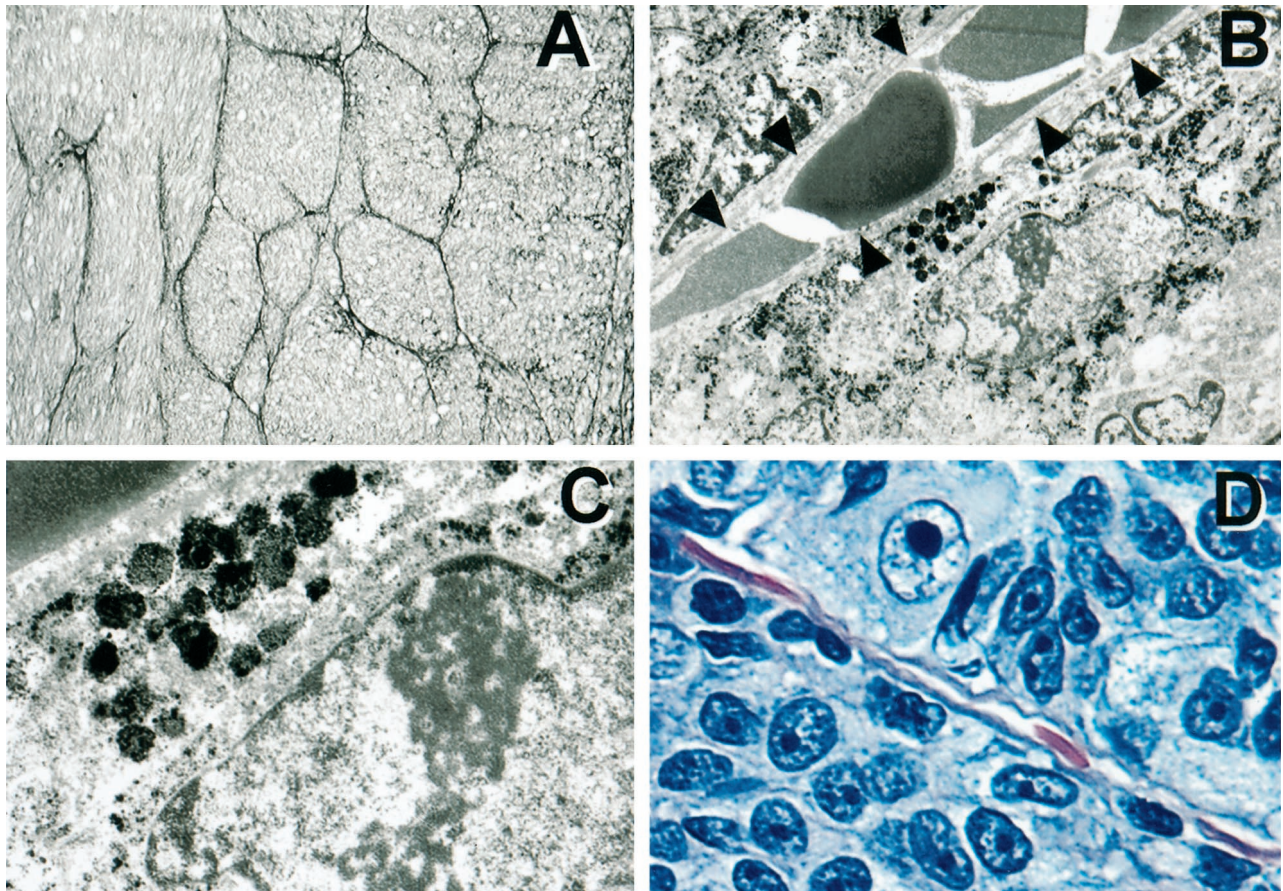
Figure 2. Transmission electron microscopy of melanoma microcirculation patterns. **A**: Tissue section of primary uveal melanoma stained by PAS without hematoxylin counterstain (same tumor as illustrated in Figure 1E). Areas from this tumor were microdissected and studied by transmission electron microscopy. **B**: Scanning magnification transmission electron micrograph of a tubule containing a single-file column of red blood cells. This vascular channel is lined by a thin basal lamina (**arrowheads**) corresponding to the walls of the channel seen by conventional light microscopy. There are no endothelial cells lining the tubule. Tumor cells containing melanosomes and premelanosomes lie external to the basal lamina. **C**: Higher magnification of Figure 2C illustrating premelanosomes and melanosomes within the tumor. **D**: Hematoxylin-eosin-stained tissue section of primary uveal melanoma. A vascular channel containing red blood cells is lined externally by tumor cells; endothelial cells are not identified. Original magnifications, ×40 (**A**), ×10,000 (**B**), ×30,000 (**C**), ×100 (**D**).

membrane structures such as Descemet's membrane, Bruch's membrane, and the internal limiting membrane of the retina.

Immunohistochemical Profile of Melanoma Intratumoral Patterned Vascular Channels

We and others had reported previously that it is possible to label PAS-positive patterns with Ulex,[7,35] Factor VIII-related antigen,[6] CD31,[6] and CD34.[31] In light of the absence of demonstrable endothelial cells by light and transmission electron microscopy in the matrix-associated vascular channels, we further evaluated the distribution of endothelial markers within these patterns.

We stained tissue sections of uveal melanomas containing abundant PAS-positive looping patterns and networks for the distribution patterns of Factor VIII-related antigen, Ulex europaeus agglutinin I, CD31, CD34, and KDR. As controls, we used either normal adjacent choroidal vasculature (which includes the fenestrated endothelium of the choriocapillaris), tissue sections of granulation tissue, or tissue sections of proliferative diabetic retinopathy—a classic example of ocular angiogenesis.

The vessels of proliferative diabetic retinopathy labeled with endothelial cell markers, such as Factor VIII-related antigen, appeared randomly clustered as discrete channels (Figure 3A) and were clearly lined by endothelial cells (Figure 3B), as demonstrated with hematoxylin counterstaining. These angiogenically derived vascular structures of proliferative diabetic retinopathy are quite different from the patterned, interconnected, looping PAS-positive channels found within aggressive melanomas (Figure 3C).

Within a given tumor, staining for endothelial cell markers such as Factor VIII-related antigen (Figure 3D) or CD31 (Figure 3E) was weak, focal, and discontinuous along the patterns, frequently leaving most of the patterns unlabeled. By contrast, the normal vessels of the surrounding choroid labeled consistently with these markers and served as an internal positive control for endothelial cells.

In portions of the patterns that failed to stain with endothelial cell markers, we frequently identified hollow tubes. Some endothelial cell markers, such as CD31, unexpectedly stained tumor cells in the vicinity of patterned tubes (Figure 3F). At high magnification, markers

Table 1. Effects of Conditioned Media and Soluble Factors on Formation of Vessels by Human Uveal Melanoma Cells

Culture designation	Cell phenotype vimentin/keratin IFs	Invasive potential	Added conditioned media (CM)/soluble factors	Vessel formation
UMEL-1 (normal choroid)	+/−	Poor (0.9 ± 0.008)	Without CM	−
			With C918 CM	−
OCM-1A (primary)	+/−	Poor (2.2 ± 0.09)	Without CM	−
			With C918 CM	−
			With M619 CM	−
			With MUM-2B CM	−
			With bFGF, TGF-β, VEGF, PDGF	−
C918 (primary)	+/+	High (12.9 ± 0.31)	Without CM	+
			With UMEL-1 CM	+
			With OCM-1A CM	+
M619 (primary)	+/+	High (12.7 ± 0.4)	Without CM	+
MUM-2B (metastasis)	+/+	High (13.3 ± 0.6)	Without CM	+

Scoring of tumor cell phenotype using classical pathology markers of vimentin (mesenchymal) and cytokeratins 8 and 18 (epithelial) intermediate filaments (IFs) was based on a positive (+) and negative (−) ranking system, determined by immunohistochemistry and/or Northern blot analysis. Invasiveness was calculated as the percentage of cells capable of invading a collagenous matrix-coated polycarbonate membrane over 24 hours within a membrane invasion culture system (MICS) compared with the total number of cells seeded (± SE; $n = 6$ wells per measurement and run in duplicate experiments). Conditioned media (CM)/soluble factors experiments were performed by treating designated 3D cultures of cells with CM from specific cell lines or exogenously added factors for 1 to 2 weeks *in vitro*, followed by microscopic scoring of vascular tube formation on 3D Matrigel or on Type I collagen gels.

such as Factor VIII-related antigen that stained the patterns were clearly seen to label the interior of the hollow lumen segmentally (Figure 3G), perhaps accounting for the discontinuous labeling seen in lower magnification (Figure 3D). We also noted that staining for endothelial cell markers such as Ulex (Figure 3H), CD34 (Figure 3I), and KDR (Figure 3J) stained the lumen contents around red blood cells within the patterns. Furthermore, when endothelial markers stained the lumen contents of the patterns, they did not stain the lumen wall, and endothelial cell nuclei were not identified within the tubes by hematoxylin counterstaining.

After double-labeling a tissue section of primary uveal melanoma with both CD31 and S-100 protein, we again did not detect staining of most of the patterns with CD31 (Figure 3K), but we did observe intense staining of cells external to the lumen of the patterned channels with S-100 protein (staining for S-100 protein is characteristic of and consistent with melanoma cells, but not with vascular endothelium; Figure 3L). In fact, staining for S-100 protein was so intense that the tumor cells outlined the negatively labeled lumen of the patterned channels (Figure 3L).

Therefore, by conventional light microscopy, transmission electron microscopy, and an immunohistochemical panel of endothelial cell markers, the looping patterned matrix-associated vascular channels of aggressive melanomas were not found to be lined by vascular endothelium.

In Vitro *Reconstitution of Patterned Matrix-Associated Vascular Channels by Cultured Aggressive Melanoma Cells*

The absence of endothelial cells lining the patterned matrix-associated vascular channels of aggressive and metastatic melanomas suggested that the melanoma cell phenotype might play a role in the generation of these patterns. To test this hypothesis, we examined the ca-pacity of melanoma cells of varying invasive and metastatic potential to recapitulate *in vitro* the network patterns seen in tissue sections in the absence of endothelial cells and fibroblasts.

Human cultures of the highly invasive M619 (Figure 4A) and C918 uveal melanoma cells, metastatic MUM-2B uveal melanoma cells (Figure 4B), and C8161 metastatic cutaneous melanoma cells (Figure 4C), all reconstituted with extraordinary fidelity the architectural patterns of loops and networks *in vitro* in gels containing Matrigel (Figure 4, A and C) or dilute Type I collagen (Figure 4B). These observations were specific for the aggressive melanoma cell phenotype, because poorly invasive OCM-1A uveal melanoma cells and normal UMEL-1 cells failed to form vessel networks *in vitro* under identical culture conditions on either Matrigel (Figure 4D) or dilute Type I collagen (Figure 4E). As in patient tissue samples, these *in vitro* tumor cell-generated patterned vascular channels were PAS-positive.

We asked whether this pattern formation was induced by a factor secreted in the conditioned medium. Addition of conditioned media from the highly invasive and metastatic cell lines (M619, C918, MUM-2B) to poorly invasive cells (OCM-1A, UMEL-1) did not result in patterned vascular channel formation (Table 1). Moreover, basic fibroblast growth factor (bFGF), transforming growth factor (TGF)-α, vascular endothelial growth factor (VEGF), platelet-derived growth factor (PDGF), and tumor necrosis factor (TNF)-α, tested individually or in combination, failed to induce formation of these networks when added to cultures of the poorly invasive cells. Similarly, no vascular channels were formed in <2% hypoxic conditions. Conversely, conditioned media from poorly invasive cells failed to inhibit *in vitro* vessel formation by highly invasive cells. Furthermore, commercially available blocking antibodies raised against $\alpha_v\beta_3$ or the α_v subunit did not inhibit patterned channel formation even at concentra-

tions exceeding a 1:20 dilution of the antibodies in culture media.
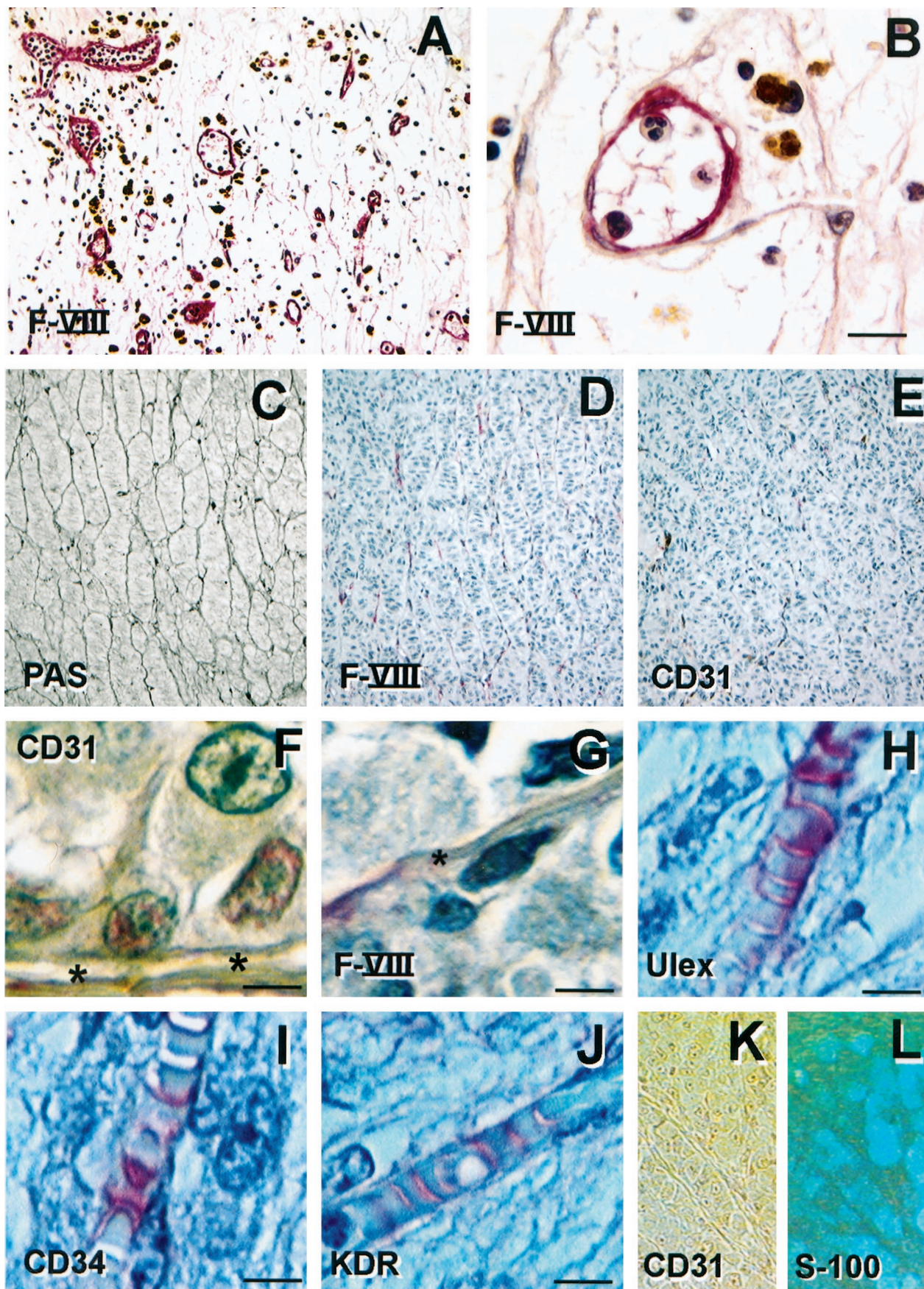
The vascular patterns formed *in vitro* (Figure 4, A-C) compartmentalized spheroidal nests of tumor cells in a fashion identical to spheroidal tumor cell nests delimited by PAS-positive microvessels observed in tissue sections from primary and metastatic melanomas (compare Figure 1, B, C, and D, with Figure 4, A-C). The structures that delimit nests of tumor cells *in vitro* are both sinusoidal and tubular, as demonstrated by histological cross-section of the cultures (Figure 4F).

We tested the perfusion characteristics of patterned tubular and sinusoidal channels generated by melanoma cells *in vitro* with the microinjection of dye into the sinusoids of mature cultures (>2 weeks). Many of these tumor-generated channels were capable of holding the injected dye and distributing it over considerable distances through the *in vitro* generated networks (Figure 4, G and H), reminiscent of the angiographic patterns seen in patients with indocyanine green angiography (Figure 1G).

Biomechanical Potential of Highly Invasive and Poorly Invasive Melanoma Cells

The invasive and metastatic uveal melanoma cell-generated patterns consisted of a phase microscopic acellular translucent tubular network embedded in the underlying cell monolayer (Figure 5A), as demonstrated by direct microdissection (Figure 5B). These channels and sinusoids evolved dynamically and anastomosed within the monolayer over a 3-day to 3-week period. Also, these networks in young cultures encircled subpopulations of tumor cells and varied widely in lumen diameter. By comparison, endothelial cell cords *in vitro* typically demonstrate a more uniform diameter on most matrices[37–40] and most, if not all, of the cultured endothelial cells typically participate in cord formation under identical media and matrix conditions without encircling subpopulations of endothelial cells (Figure 5C). The presence of spheroidal cell nests within the boundaries formed by tumor cell cords is not a characteristic feature of endothelial cord formation in Matrigel or on other matrices (compare Figure 5A with Figure 5C). Therefore, the presence of spheroidal nests of melanoma cells encircled by patterned, acellular hollow tubes in pure tumor cultures constitutes a major difference between tumor and endothelial cord formation under identical conditions.

The potential of many cell types to generate cords, tessellations, and tube-like structures *in vitro* has been linked to their ability to constrict and remodel matrix fibers.[38,41] In addition, highly invasive melanoma cells have been demonstrated to contract floating collagen gels.[42] Because we observed that highly invasive melanoma cells could generate patterned vessels *in vitro*, we explored the ability of these cells to contract floating matrices as evidence of their matrix remodeling potential.

First, we compared the ability of cultured melanoma cells of varying phenotypes with that of endothelial cells to contract gels during similar time periods with identical gel densities and media conditions. Endothelial cells contracted floating collagen gels within 48 hours (Figure 5D). Highly invasive C918 primary uveal melanoma cells and metastatic C8161 cutaneous melanoma cells all constricted floating collagen gels in a similar fashion within 48 hours (Figure 5, E and F). In contrast, poorly invasive OCM-1A primary uveal melanoma cells did not constrict the gels at all, and tension lines were not observed anywhere in the gel (Figure 5G), even after 3 weeks. Finally, when the gels were stained with a variety of vital dyes that label mitochondria, we noted that only the aggressive melanoma cell lines formed network patterns as they contracted the gels (Figure 5H).

Next, we tested whether drugs that block the ability of actin microfilaments to transduce forces throughout the cell could block gel contraction reversibly.[24] By targeting actin, we found that the ability of highly invasive and metastatic cells to constrict matrices was blocked with 1 μmol/L cytochalasin-D and that this effect was reversible on removal of the drug (gels were observed to contract after the media was replaced and the drug removed; data not shown). Thus, the biomechanical ability of cells to remodel matrices, a mechanical prerequisite for tube formation, is linked to the invasive and metastatic tumor cell phenotype and does not occur with poorly invasive cells.

Figure 3. Immunohistochemistry of melanoma microcirculation patterns. **A:** Proliferative diabetic retinopathy, a classic example of an angiogenic response, was used as one control. The discrete vessels stained for Factor VIII-related antigen are not interconnected and do not form loops that encircle domains of tissue in histological section (as shown in Figure 1, A-E and H). **B:** Higher magnification of proliferative diabetic retinopathy stained for Factor VIII-related antigen. At least five endothelial cell nuclei are identified lining this small vessel. Cells containing brown pigment represent iron in macrophages and reflects vascular incompetence in this neo-angiogenic response. **C:** Tissue section taken from primary uveal melanoma, stained by PAS without hematoxylin. This patient died of metastatic melanoma. Note the interconnected loops. **D:** Same tumor as illustrated in **C**, stained for Factor VIII-related antigen (appears red). The loops stain only focally and discontinuously. **E:** The same tumor as illustrated in **C** and **D**, stained for CD31. Staining of this pattern with CD31 is even less evident than with Factor VIII-related antigen. **F:** Primary uveal melanoma showing intense CD31 staining (appears red) of tumor cells adjacent to the lumen (*) of intratumoral vascular tube lacking endothelial lining. This patient died of metastasis 6 years after the eye was removed. **G:** Higher magnification of tumor depicted in **D**, also stained for Factor VIII-related antigen. Only a segment of this otherwise hollow channel (*) stains for Factor VIII-related antigen. The remainder of the tube is vacant (*). Endothelial cell nuclei are not identified. **H:** Tissue section stained by Ulex europaeus agglutinin I (appears red) and counterstained with hematoxylin. Endothelial cell nuclei are not identified. Ulex labels the contents of the lumen around the red blood cells. Tumor cells are identified external to the vessel. **I:** Tissue section stained with CD34 and counterstained with hematoxylin; endothelial cell nuclei are not identified. CD34 labels the lumen contents between the red blood cells. Tumor cells are situated external to the vessel. **J:** Tissue section stained for KDR (appears red) and counterstained with hematoxylin; endothelial cell nuclei are not identified. The lumen contents are labeled with KDR. Tumor cells are situated external to the vascular channel. **K:** Tissue section double labeled for CD31 (red chromogen with direct illumination) and **L,** S-100 protein (same field viewed by reflectance microscopy; immunogold). The vascular channels do not stain for CD31 but cells apposed externally to the vascular channel lumen are positive for S-100 protein, a reaction consistent with melanoma, but not endothelial cells. Tissue stains: **A, B, D,F,** Factor VIII-related antigen, counterstained with hematoxylin; **C,** PAS without hematoxylin counterstain; **E** and **G,** CD31 counterstained with hematoxylin; **H,** Ulex europaeus agglutinin I counterstained with hematoxylin; **I,** CD34, counterstained with hematoxylin; **J,** KDR, counterstained with hematoxylin; **K,** CD31 (red chromogen) photographed by direct illumination; **L,** S-100 protein conjugated to immunogold (same section, same field as **K**) photographed with epipolarization microscopy. Original magnifications, ×20 (**A, C, D, E, K,** and **L**). Scale bar, 25 μm for **B,F,G,** and **H.**
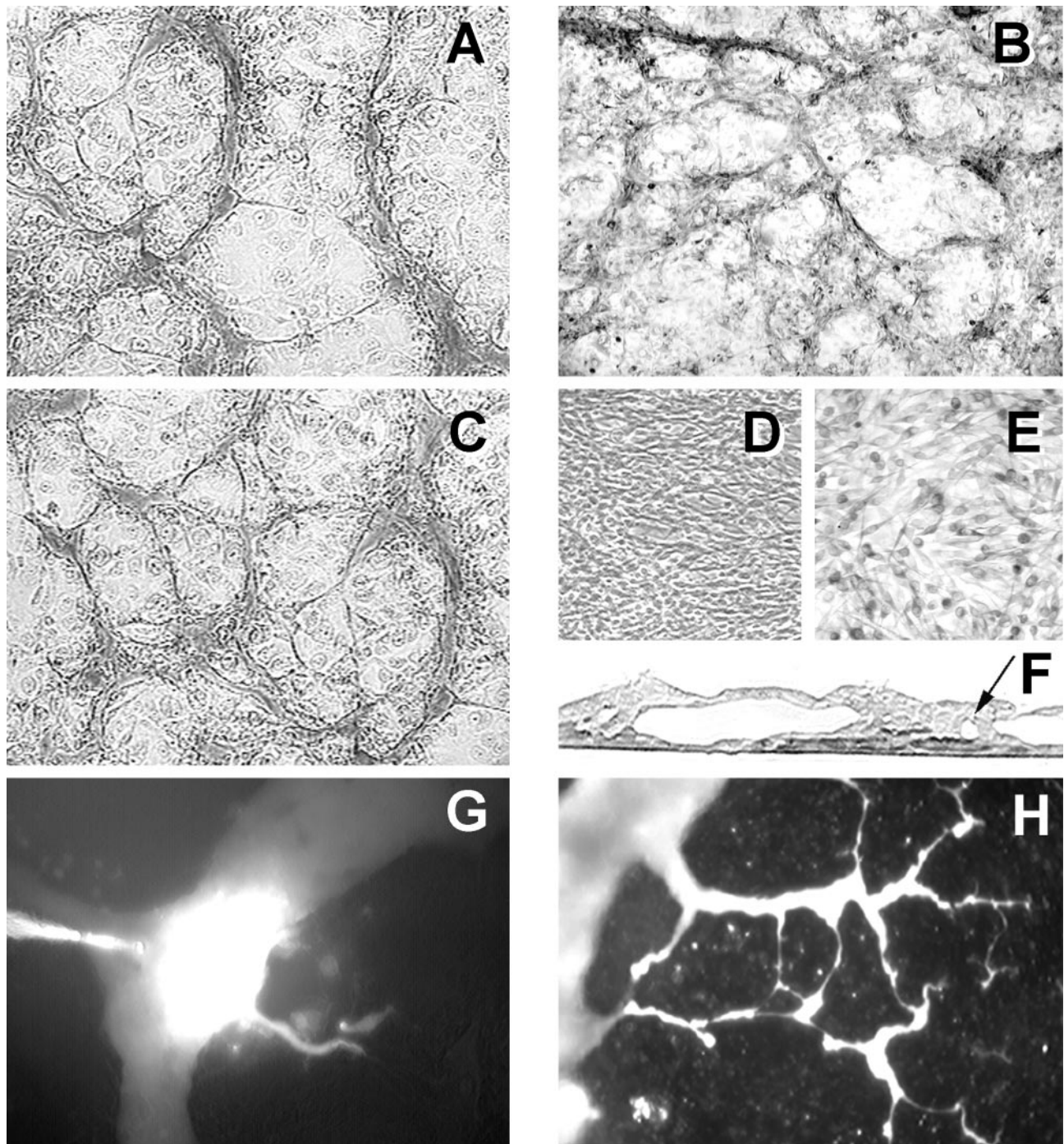
Figure 4. A: PAS-stained phase contrast micrograph of 3D culture of highly invasive M619 human uveal melanoma cells forming patterned networks after 1 week on Matrigel. **B**: Metastatic uveal melanoma MUM-2B forming patterned networks on dilute Type I collagen (stained with PAS to highlight basement membranes). **C**: Metastatic cutaneous melanoma C8161 also formed patterned networks after 1 week on Matrigel. By contrast, poorly invasive OCM-1A cells do not form patterned networks on Matrigel (**D**) or on dilute Type I collagen gels (**E**). **F**: Histological cross-section of a 2-week, 3D culture of cell line M619 showing both large sinusoidal structures and smaller tubular structures embedded in the monolayer (**arrow**). **G**: Fluorescence localization of Texas red dye at the moment of microinjection into a large sinusoid of a mature vessel-forming 3D culture of pure MUM-2B cells. **H**: The dye distributes through smaller tumor-generated vessels in 30 minutes. Compare with Figure 1G, the confocal angiogram taken of a patient with a uveal melanoma. Original magnifications, ×200 (**F**); ×40 (all others).

cDNA Microarray Analysis: Comparison between Poorly Invasive and Highly Invasive Melanoma Cells

We compared poorly invasive and highly invasive uveal melanoma cells derived from the same patient using hybridization to cDNA microarrays.[26,43] This approach allowed the expression analysis of 5000 genes simultaneously. Comprehensive results will be provided elsewhere, but, as illustrated in Table 2, numerous genes whose expression patterns were altered in association with the invasive phenotype further validated our histo-
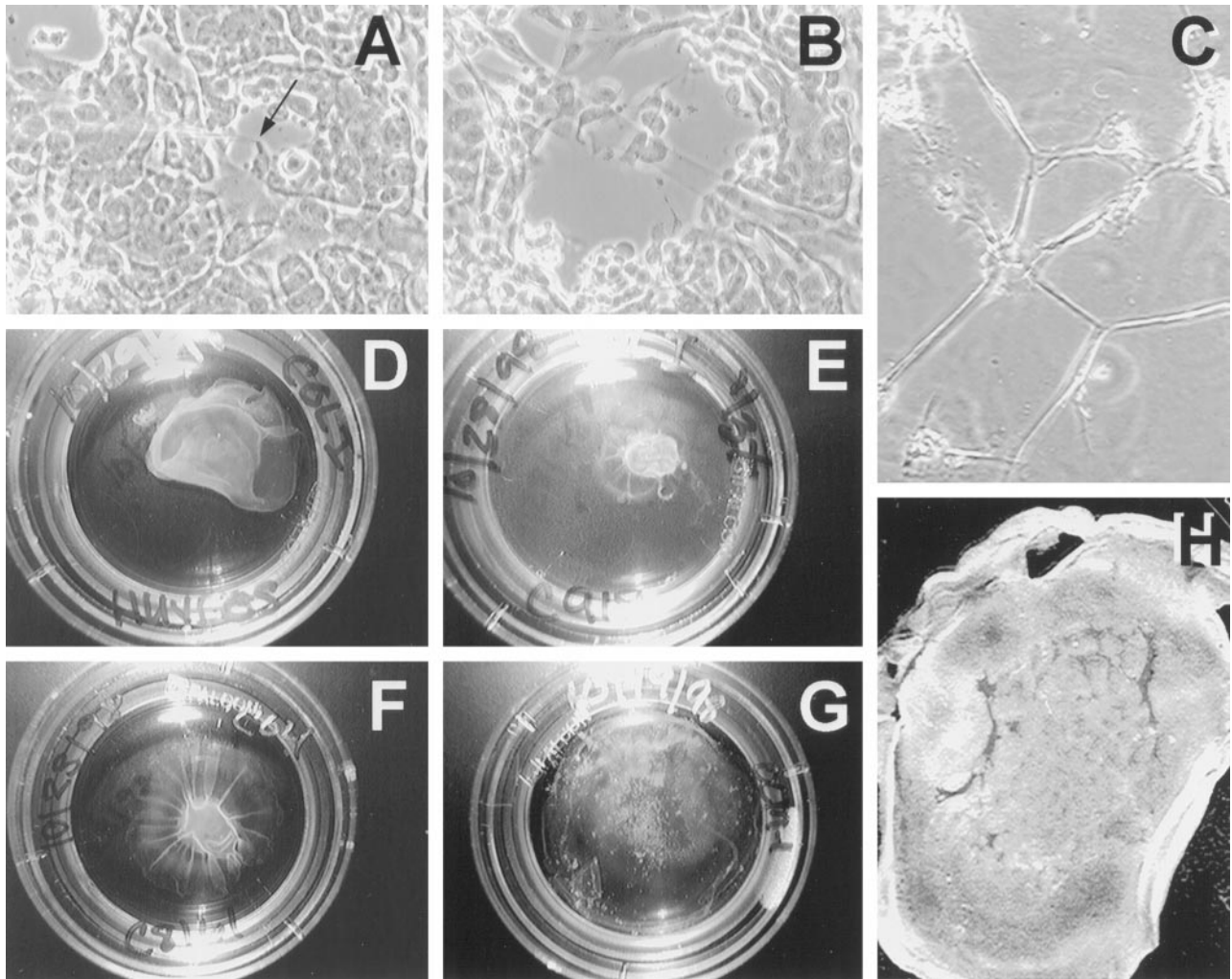
Figure 5. Physical and deregulated characteristics of uveal melanoma vessels. A: Micromanipulation of a tumor-generated vessel formed by M619 melanoma cells and removal of cells (**small black arrow**) from the acellular vascular channel, and all others. B: subsequent deformation of the same tubular structure for measurement of its mechanical response to applied strain.[24] C: Cord formation by cultured human endothelial cells under identical media and culture conditions shown in A and B. Note that all of the endothelial cells are recruited into tessellations, unlike spheroidal nests of aggressive cultured melanoma cells which are encircled by acellular microvessels of varying diameters (A and B). D-G: Comparison of collagen gel contraction after seeding with HUVECs or tumor cells. Endothelial cells (D) contracted the floating gels in 48 hours, as do aggressive primary C918 intraocular melanoma cells (E) and metastatic C8161 cutaneous melanoma cells (F); however, poorly invasive OCM-1A primary melanoma cells (G) did not contract the floating gels even after 3 weeks' observation. H: Concomitant gel contraction and tube formation on floating hydrated gel. Highly invasive M619 melanoma cells contract the gel and form networks as demonstrated by labeling of tumor cell mitochondria with rhodamine 123.

logical and *in vitro* observations. Briefly summarized, of the 210 known genes that were differentially expressed in these tumor populations, approximately 15 have been associated previously with the endothelial/vascular phenotype. Examples include tyrosine kinase with immunoglobulin and epidermal growth factor homology domains (TIE-1), an endothelial receptor kinase involved in vessel formation and maturation,[44] urokinase-type plasminogen activator (uPA), epithelial cell kinase (ECK),and keratin 8 intermediate filament, which collectively support the deregulated embryonic-like phenotype displayed by the highly invasive melanoma cells.[45] A series of genes that would generate relevant biological molecules to form microvascular channels were also observed to be overexpressed in the aggressive melanoma cells including connective tissue growth factor (CTGF), the extracellular matrix-associated fibrillin, collagens VI[17] and I, and fi-

bronectin. Genes shown to be underexpressed in the highly invasive cells included myosin light-chain kinase, whose deregulation product might alter actomyosin interactions. In summary, the cDNA microarray analysis of highly invasive *versus* poorly invasive melanoma tumor cells confirmed a genetic reversion to a pluripotent embryonic-like genotype in the highly aggressive melanoma cells.

Discussion

Until now, it has been taken for granted that all intratumoral vascular channels are formed and lined by endothelial cells. The demonstration that human melanoma cells containing melanosomes and premelanosomes are found lining patterned vascular channels in patients' pri-

Table 2. Microarray Analysis of Highly Invasive/Metastatic *versus* Poorly Invasive Uveal Melanoma Cells

Protein	Symbol	Unigene	Function	Ratio*
Endothelial receptor kinase	TIE-1	Hs.78824	Receptor tyrosine kinase	>100
Urokinase-type plasminogen activator	PLAU	Hs.77274	Proteolysis	80
Epithelial cell kinase	ECK	Hs.32197	Receptor tyrosine kinase	77
Connective tissue growth factor	CTGF	Hs.75511	Growth factor	35
Keratin 8	KRT8	Hs.78271	Intermediate filament	18
Fibrillin	FNB1	Hs.750	Extracellular matrix	12
Collagen VI	COL6A1	Hs.80988	Extracellular matrix	6.7
Fibronectin	FN1	Hs.100056	Extracellular matrix	4.2
Collagen I, α-2	COL1A2	Hs.90283	Extracellular matrix	2.5
Myosin light chain kinase	MYLK	Hs.75950	Regulator of contractility	0.12

Altered gene expression in human uveal melanoma cells was identified by cDNA microarray analysis.
*Relevant expression of selected genes significant for vascular channel formation is reported as the ratio of highly invasive and metastatic to poorly invasive uveal melanoma cells.

mary and metastatic tumors, and that these tumor cells generate a functional perfusable network *in vitro*, calls for reappraisal of the current assumption that endothelial cell-mediated angiogenesis is the only mechanism underlying or responsible for tumor growth and metastasis.

Our observations address the intriguing cellular and molecular mechanisms underlying the formation of patterned vascular channels found in the most aggressive primary intraocular (uveal) melanomas and their metastases and in metastatic cutaneous melanomas. The data reveal that: (i) the patterned vascular channels of aggressive primary and metastatic melanoma are different from endothelial-derived angiogenic vessels; (ii) highly invasive melanoma cells, but not poorly invasive ones, reconstitute the patterned vascular channels seen in human tumor tissue *in vitro* in the absence of endothelium; (iii) the tumor cells that generate the patterned vascular channels are deregulated and aberrantly express genes heretofore associated with embryonic stem cells including those associated with primordial vascular development; and (iv) the generation of patterned vascular channels by deregulated aggressive tumor cells in human melanomas is a novel pathway to generate microcirculation in a tumor and facilitate metastasis.

The patterned vascular channels characteristic of aggressive primary and metastatic melanoma are different from angiogenic vessels in that (i) vascular channels in aggressive melanomas are embedded in highly patterned matrix (Figure 1, B-D), whereas angiogenic vessels (the growth of new blood vessels from a pre-existing microcirculation) are characterized by clusters of vessels and are not patterned (Figure 3, A and B); (ii) the patterned melanoma vascular channels were not found to be lined by endothelium by light microscopy (Figures 1E, 2B, and 3, F-L), transmission electron microscopy (Figure 2, B and C), and immunohistochemistry (Figure 3, D-L), whereas the contribution of an endothelium to angiogenic vessels in proliferative diabetic retinopathy and normal vessels in the adjacent normal tissue is clearly identified by light microscopy and immunohistochemistry (Figure 3, A and B); and (iii) the architecture of the matrix-associated vascular channels, characterized by interconnected loops and networks, although not typical of angiogenesis, is characteristic of vasculogenesis (formation of networked microvasculature by incorporation of cells).[2]

Highly invasive melanoma cells reconstitute *in vitro* the patterned matrix-associated vascular channels seen in human melanomas in the absence of endothelial cells and fibroblasts. In contrast, poorly invasive melanoma cells are not capable of generating the biomechanical properties (ie, capable of contracting matrices) required to generate patterned acellular vascular channels *in vitro*. The ability of highly invasive, but not poorly invasive, melanoma cells to generate patterned vascular channels *in vitro* helps to explain the very strong association between the presence of the vascular channel-associated patterns in patient tissues and death from metastatic melanoma (Figure 1F).[4]

The formation of a microcirculation by cells other than endothelial cells has been reported in normal embryonic tissues, but not previously in the context of tumor progression. For example, there is strong evidence suggesting that human cytotrophoblasts adopt an endothelial cell phenotype as they participate in the establishment of the human placenta and primordial microcirculation.[46–48] Indeed, invasive melanoma cells capable of generating a patterned microcirculation *in vitro* express inappropriate markers. For example, we previously showed that highly invasive and metastatic melanoma cells (but not poorly invasive cells) express embryonic keratins in addition to their classical vimentin intermediate filament marker.[45] Moreover, highly invasive, but not poorly invasive, melanoma cells express the c-*met* proto-oncogene and demonstrate responsiveness to scatter factor (HGF/SF), a potent mitogen, morphogen, and motogen.[49] Finally, cDNA microarray analysis, comparing poorly invasive with highly invasive melanoma cells, discloses a variety of differential gene expression associated with a combination of phenotypes including endothelium (TIE-1) and epithelium (keratin 8), suggesting a genetic reversion to a pluripotent embryonic-like phenotype. The ability of highly invasive melanoma cells to generate patterned vascular channels may be one of many important pluripotent manifestations of this embryonic-like phenotype, which ensures remodeling, perfusion, tumor cell viability, and a dissemination mechanism.

Analysis of differential gene expression between highly and poorly invasive melanoma cells supports our observation that highly invasive cells generate a patterned paracirculation *in vitro*. The underexpression of myosin

light chain kinase,[50] a regulator of contractility, in highly invasive melanoma cells is consistent with the differential ability of these, but not of poorly invasive melanoma cells, to contract matrices and form a patterned paracirculation (Figures 4 and 5).

Our data suggest that tumor cell-generated vascular channels provide a blood supply required for growth and metastasis without the influence of soluble tropic factors associated with stimulated angiogenesis in other contexts, such as diabetic retinopathy in the eye. The generation of highly patterned and functional vascular channels by the tumor itself is a marker of the aggressive tumor cell phenotype. The generation of the patterned melanoma microcirculation is vasculogenic mimicry mediated by the tumor cells themselves and may function independently of tumor angiogenic mechanisms during various phases of tumor progression. Therefore, the unique observations reported here should serve as a catalyst for exploring patterned vascular channel formation in other tumors and may provide new clues for the development of novel treatment modalities that target the molecular basis for the unique architecture of the tumor-generated microcirculation.[51,52]

Acknowledgments

References

1. Folkman J: Clinical applications of research on angiogenesis. Seminars in Medicine of the Beth Israel Hospital, Boston. New Engl J Med 1995, 333:1757–1763
2. Risau W: Mechanisms of angiogenesis. Nature 1997, 386:671–674
3. Weidner N: Tumoral vascularity as a prognostic factor in cancer patients: the evidence continues to grow. J Pathol 1998, 184:119–122
4. Folberg R, Rummelt V, Parys-Van Ginderdeuren R, Hwang T, Woolson RF, Pe'er J, Gruman LM: The prognostic value of tumor blood vessel morphology in primary uveal melanoma. Ophthalmology 1993, 100:1389–1398
5. McLean IW, Foster WD, Zimmerman LE, Gamel JW: Modifications of Callender's classification of uveal melanoma at the Armed Forces Institute of Pathology. Am J Ophthalmol 1983, 96:502–509
6. Folberg R, Mehaffey M, Gardner LM, Meyer M, Rummelt V, Pe'er J: The microcirculation of choroidal and ciliary body melanomas. Eye 1997, 11:227–238
7. Folberg R, Pe'er J, Gruman LM, Woolson RF, Jeng G, Montague PR, Moninger TO, Yi H, Moore KC: The morphologic characteristics of tumor blood vessels as a marker of tumor progression in primary human uveal melanoma: a matched case-control study. Hum Pathol 1992, 23:1298–1305
8. McLean IW, Keefe KS, Burnier MN: Uveal melanoma: comparison of the prognostic value of fibrovascular loops, mean of the ten largest nucleoli, cell type and tumor size. Ophthalmology 1997, 104:777–780
9. Pe'er J, Rummelt V, Mawn L, Hwang T, Woolson RF, Folberg R: Mean of the ten largest nucleoli, microcirculation architecture, and prognosis of ciliochoroidal melanomas. Ophthalmology 1994, 101:1227–1235
10. Mehaffey MG, Folberg R, Meyer M, Bentler SE, Hwang T, Woolson RF, Moore KC: Relative importance of quantifying area and vascular patterns in uveal melanoma. Am J Ophthalmol 1997, 123:798–809
11. Bartsch D-U, Weinreb RN, Zinser G, Freeman WR: Confocal scanning infrared laser ophthalmoscopy for indocyanine green angiography. Am J Ophthalmol 1995, 120:642–651
12. Schneider U, Gelisken F, Inhoffen W, Kreissig I: Indocyanine-green videoangiography of malignant melanomas of the choroid using the scanning laser ophthalmoscope. Ger J Ophthalmol 1996, 5:6–11
13. Mueller AJ, Bartsch DU, Folberg R, Mehaffey MG, Boldt HC, Meyer M, Gardner LM, Goldbaum MH, Peer J, Freeman WR: Imaging the microvasculature of choroidal melanomas with confocal indocyanine green scanning laser ophthalmoscopy. Arch Ophthalmol 1998, 116:31–39
14. Folberg R, Verdick RE, Weingeist TA, Montague PR: Gross examination of eyes removed for ciliary body or choroidal melanoma. Ophthalmology 1986, 93:1643–1647
15. Hendrix MJ, Seftor EA, Seftor RE, Trevor KT: Experimental co-expression of vimentin and keratin intermediate filaments in human breast cancer cells results in phenotypic interconversion and increased invasive behavior. Am J Pathol 1997, 150:483–495
16. Rummelt V, Mehaffey MG, Campbell RJ, Peer J, Bentler SE, Woolson RF, Naumann GOH, Folberg R: Microcirculation architecture of metastases from primary ciliary body and choroidal melanomas. Am J Ophthalmol 1998, 126:303–305
17. Daniels KJ, Boldt HC, Martin JA, Gardner LM, Meyer M, Folberg R: Expression of Type VI collagen in uveal melanoma: role in pattern formation and tumor progression. Lab Invest 1996, 75:55–66
18. Welch DR, Bisi JE, Miller BE, Conaway D, Seftor EA, Yohem KH, Gilmore LB, Seftor RE, Nakajima M, Hendrix MJ: Characterization of a highly invasive and spontaneously metastatic human malignant melanoma cell line. Int J Cancer 1991, 47:227–237
19. Stamer WD, Huang Y, Seftor RE, Svensson SS, Snyder RW, Regan JW: Cultured human trabecular meshwork cells express functional α 2A adrenergic receptors. Invest Ophthalmol Vis Sci 1996, 37:2426–2433
20. Seftor EA, Seftor REB, Way DL, Bernas M, Weinland CL, Witte CL, Witte MH, Hendrix MJC: Enhancement of endothelial cell and Kaposi sarcoma migration by selective chemoattractants. Lymphol 1994, 27:755–758 (suppl)
21. Xu Y, Swerlick RA, Sepp N, Bosse D, Ades EW, Lawley TJ: Characterization of expression and modulation of cell adhesion molecules on an immortalized human dermal microvascular endothelial cell line (HMEC-1). J Invest Dermatol 1994, 102:833–837
22. Hendrix MJ, Seftor EA, Seftor RE, Fidler IJ: A simple quantitative assay for studying the invasive potential of high and low human metastatic variants. Cancer Lett 1987, 38:137–147
23. Hendrix MJC, Seftor EA, Chu YW, Trevor KT, Seftor REB: Role of intermediate filaments in migration, invasion and metastasis. Cancer Metastasis Rev 1996, 15:507–525
24. Maniotis A, Chen C, Ingber D: Demonstration of mechanical interconnections between integrins, cytoskeletal filaments, and nuclear scaffolds that stabilize nuclear structure. Proc Natl Acad Sci USA 1997, 94:849–854
25. Eckes B, Dogic D, Colucci-Guyon E, Wang N, Maniotis A, Ingber D, Merckling A, Langa F, Aumailley M, Delouvee A, Kotellansky V, Babinet C, Kreig T: Impaired mechanical stability, migration and contractile capacity in vimentin-deficient fibroblasts. J Cell Sci 1997, 94:1897–1907
26. DeRisi J, Penland L, Brown PO, Bittner ML, Meltzer PS, Ray M, Chen Y, Su YA, Trent JM: Use of a cDNA microarray to analyse gene expression patterns in human cancer [see comments]. Nat Genet 1996, 14:457–460
27. Khan J, Simon R, Bittner M, Chen Y, Leighton SB, Pohida T, Smith PD, Jiang Y, Gooden GC, Trent JM, Meltzer PS: Gene expression profiling

of alveolar rhabdomyosarcoma with cDNA microarrays. Cancer Res 1998, 58:5009–5013

28. Schuler GD, Boguski MS, Stewart EA, Stein LD, Gyapay G, Rice K, White RE, Rodriguez-Tome P, Aggarwal A, Bajorek E, Bentolila S, Birren BB, Butler A, Castle AB, Chiannilkulchai N, Chu A, Clee C, Cowles S, Day PJ, Dibling T, Drouot N, Dunham I, Duprat S, East C, Hudson TJ: A gene map of the human genome. Science 1996, 274:540–546

29. McLean IW: The biology of haematogenous metastasis in human uveal malignant melanoma. Virchows Arch A Pathol Anat 1993, 422: 433–437

30. Sakamoto T, Sakamoto M, Yoshikawa H, Hata Y, Ishibashi T, Ohnishi Y, Inomata H: Histologic findings and prognosis of uveal malignant melanoma in Japanese patients. Am J Ophthalmol 1996, 121:276–283

31. Makitie T, Summanen P, Tarkannen A, Kivela T: Microvascular loops and networks as prognostic indicators in choroidal and ciliary body melanomas. J Natl Cancer Inst 1999, 91:359–367

32. Rummelt V, Folberg R, Rummelt C, Gruman LM, Hwang T, Woolson RF, Yi H, Naumann GOH: Microcirculation architecture of melanocytic nevi and malignant melanomas of the ciliary body and choroid. A comparative histopathologic and ultrastructural study. Ophthalmology 1994, 101:718–727

33. Folberg R, Fleck M, Mehaffey MG, Meyer M, Bentler SE, Woolson RF, Pe'er J: Mapping prognostically significant vascular patterns in ciliary body and choroidal melanomas. Pathol Oncol Res 1996, 2:229–236

34. Mehaffey MG, Gardner LM, Folberg R: Distribution of prognostically important vascular patterns across multiple levels in ciliary body and choroidal melanomas. Am J Ophthalmol 1998, 126:373–378

35. Rummelt V, Gardner LM, Folberg R, Beck S, Knosp B, Moninger TO, Moore KC: Three-dimensional relationships between tumor cells and microcirculation using double cyanine-immunolabeling, laser scanning confocal microscopy and computer-assisted reconstruction: an alternative to cast corrosion preparations. J Histochem Cytochem 1994, 42:681–686

36. Silverman RH, Folberg R, Boldt HC, Rondeau MJ, Lloyd HO, Mehaffey MG, Lizzi FL, Coleman DJ: Correlation of ultrasound parameter imaging with microcirculatory patterns in uveal melanomas. Ultrasound Med Biol 1997, 23:573–581

37. Folkman J, Haudenschild C: Angiogenesis in vitro. Nature 1980, 288:551–556

38. Ingber DE, Folkman J: Mechanochemical switching between growth and differentiation during fibroblast growth factor-stimulated angiogenesis in vitro: role of extracellular matrix. J Cell Biol 1989, 198:317–330

39. Nicosia RF, Ottinetti A: Modulation of microvascular growth and morphogenesis by reconstituted basement membrane gel in three-dimensional cultures of rat aorta: a comparative study of angiogenesis in matrigel, collagen, fibrin, and plasma clot. In Vitro Cell Dev Biol 1990, 26:119–128

40. Vernon RB, Sage EH: Between molecules and morphology: extracellular matrix and creation of vascular form. Am J Pathol 1995, 147: 873–883

41. Vernon RB, Lara SL, Drake CJ, Iruelaarispe ML, Angello JC, Little CD, Wight TN, Sage EH: Organized type I collagen influences endothelial patterns during spontaneous angiogenesis in vitro: planar cultures as models of vascular development. In Vitro Cell Dev Biol Anim 1995, 31:120–131

42. Klein CE, Dressel D, Steinmayer T, Mauch C, Eckes B, Krieg T, Bankert RB, Weber L: Integrin $\alpha 2\beta 1$ is upregulated in fibroblasts, and highly aggressive melanoma cells in three-dimensional collagen lattices, and mediates the reorganization of collagen I fibrils. J Cell Biol 1991, 115:1427–1436

43. Khan J, Simon R, Bitner M, Chen Y, Leighton SB, Poheida T, Smith P, Jiang U, Gooden JC, Trent JM, Meltzer PS: Gene expression profiling of alveolar rhabdomyosarcoma with cDNA microarrays. Cancer Res 1998, 58:5009–5013

44. McCarthy MJ, Crowther M, Bell PR, Brindle NP: The endothelial receptor tyrosine kinase tie-1 is upregulated by hypoxia and vascular endothelial growth factor. FEBS Lett 1998, 423:334–338

45. Hendrix MJC, Seftor EA, Seftor RB, Gardner LM, Boldt HC, Meyer M, Peer J, Folberg R: Biologic determinants of uveal melanoma metastatic phenotype - role of intermediate filaments as predictive markers. Lab Invest 1998, 78:153–163

46. Zhou Y, Damsky CH, Fisher SJ: Preeclampsia is associated with failure of human cytotrophoblasts to mimic a vascular adhesion phenotype: one cause of defective endovascular invasion in this syndrome? J Clin Invest 1997, 99:2152–2164

47. Zhou Y, Fisher SJ, Janatpour M, Genbacev O, Dejana E, Wheelock M, Damsky CH: Human cytotrophoblasts adopt a vascular phenotype as they differentiate: a strategy for successful endovascular invasion? J Clin Invest 1997, 99:2139–2151

48. Damsky CH, Fisher SJ: Trophoblast pseudo-vasculogenesis: faking it with endothelial adhesion receptors. Curr Opin Cell Biol 1998, 10: 660–666

49. Hendrix MJC, Seftor EA, Seftor REB, Gardner LM, Boldt HC, Meyer M, Pe'er J, Folberg R: Regulation of uveal melanoma interconverted phenotype by hepatocyte growth factor/scatter factor (HGF/SF). Am J Pathol 1998, 152:855–863

50. Fujita K, Ye LH, Sato M, Okagaki T, Nagamachi Y, Kohama K: Myosin light chain kinase from skeletal muscle regulates an ATP-dependent interaction between actin and myosin by binding to actin. Mol Cell Biochem 1999, 190:85–90

51. Ruoslahti E, Engvall E: Integrins and vascular extracellular matrix assembly. J Clin Invest 1997, 100:S53–S56

52. Arap W, Pasqualini R, Ruoslahti E: Cancer treatment by targeted drug delivery to tumor vasculature in a mouse model. Science 1998, 279: 377–380